Master's thesis

NTNU
Norwegian University of Science and Technology
Faculty of Natural Sciences
Department of Chemical Engineering

Askild Johannes Balchen Lønning

Fabrication and Characterization of Polymeric Membranes for Dehydration of Triethylene Glycol Used for Subsea Application

Master's thesis in Chemical engineering and Biotechnology
Supervisor: Liyuan Deng, IKP
January 2019

NTNU
Norwegian University of
Science and Technology

Askild Johannes Balchen Lønning

Fabrication and Characterization of Polymeric Membranes for Dehydration of Triethylene Glycol Used for Subsea Application

Master's thesis in Chemical engineering and Biotechnology
Supervisor: Liyuan Deng, IKP
January 2019

Norwegian University of Science and Technology
Faculty of Natural Sciences
Department of Chemical Engineering

Preface

This thesis is the final work of the master programme in Chemical Engineering at the Norwegian University of Science and Technology NTNU.

I would like to express my thanks to my supervisor Associate Professor Liyuan Deng and my co-supervisor Phd Candidate Mahdi Ahmadi for providing the project and for invaluable help and guidance throughout this project.

Abstract

The purpose of this project was to determine the viability of using a polybenzimidazole (PBI) membrane for the dehydration of triethylene glycol, (TEG), as a regeneration step for the TEG in a membrane process for dehydrating natural gas. This is part of a project for SUBPRO which is a centre for innovation based research within subsea production and processing[1].

The remote locations and weather conditions at possible natural gas deposits often means that a dehydration process on a platform is not viable. Due to this fact there are many new projects that are investigating the possibility of moving these processes to the seafloor. It is not viable to install the traditional natural gas dehydration processes at the seafloor due to problems with operations and maintenance and a membrane dehydration process utilizing a membrane contactor and a membrane pervaporator with TEG as an absorbent has therefore been proposed by SUBPRO as a possible solution[1]. This project concerns the pervaporation part of this membrane dehydration process.

A PBI membrane was prepared with a $2{,}5 \pm 0{,}2 \mu m$ thick layer of PBI and a $25 \mu m$ thick porous polypropylene support by knife casting and tested in a pervaporation setup with a TEG/water solution on the feed side at different water concentrations. The membrane was characterized by the use of TGA, SEM, optical tensiometer and GC.

The membrane showed no TEG uptake during the sorbtion tests wich can be seen as an indication that the membrane is suitable for the dehydration of TEG. The separation factor was also shown to be quite good, however there were problems with the results from the gas chromatograph due to condensation of TEG in the membrane setup which means that the separation factor is probably highly inaccurate. More studies will therefore have to be done with this membrane to determine the actual TEG permeance and the selectivity to make any concrete conclusions about the separation performance of this membrane, however the water permeance and flux values were not affected drastically by the inaccurate TEG concentrations and from these calculations it can be said that the membrane shows promise as a membrane for the dehydration of TEG.

Sammendrag

Hensikten med dette prosjektet er undersøke om en polybenzimidazole (PBI) membran kan brukes til å dehydrere trietylen glykol (TEG) i en pervaporasjonsprosess som en del av en membranprosess for dehydrering av naturgass. Dette prosjektet er en del av et prosjekt av SUBPRO som er et senter for innovasjonsbasert forskning innen subsea produksjon og prosessering[1].

Siden mange nye gassreservoarer blir funnet på mer avsideliggende steder med harde værforhold vil det ikke være praktisk å bruke en platform for å dehydrere naturgassen på overflaten. Det er derfor mange nye forskningsprosjekter som ser på muligheten for å plasere behandlingen av naturgassen på havbunnen. Limitasjoner på de mer tradisjonelle dehydreringsprosessene gjør at det ikke er mulig å implementere dem på havbunnen og det er derfor blitt foreslått en membranprosess som bruker en kombinasjon av en membran kontaktor og en membran pervaporator for å løse dette problemet[1]. Dette prosjektet ser på pervaporasjonsdelen av denne prosessen.

Membranen viste ingen absorbsjon av TEG ved absorbsjonstester og er derfor et lovende material for dehydrering av TEG. Den beregnede separasjonsfaktoren var svært god, men det var problemer med målingen av TEG konsentrasjonen med gaskromatograf og separasjonsfaktoren er derfor mest sannsynlig svært unøyaktig. Det trengs derfor flere tester der disse problemene er løst for å kunne komme til en konklusjon om separasjonsfaktoren og permeabiliteten til TEG. TEG konsentrasjonene var så lav at det ikke hadde en signifikant innvirkning på permeabiliteten og fluksen til vann og disse målingene viser til at PBI er en lovende membran for dehydrering av TEG.

Contents

Introduction **1**
1.1 Motivation . . . 1
1.1.1 Research objectives . . . 2

Theory **4**
2.1 Natural gas dehydration. . . . 4
2.2 Subsea natural gas processing . . . 5
2.3 Membrane dehydration . . . 6
2.4 Membrane pervaporation . . . 7
2.5 Membrane materials and membrane types for pervaporation . . . 8
2.5.1 Solution-Diffusion model . . . 9
2.5.2 Free volume theory . . . 10
2.5.3 Membrane pervaporation theory . . . 11

Experimental **14**
3.1 Membrane materials . . . 14
3.2 Membrane preparation . . . 14
3.3 Contact angle measurements . . . 14
3.4 TEG sorbtion tests . . . 15
3.5 Membrane morphology . . . 15
3.6 Gas chromatography . . . 15
3.6.1 Gas chromatography test preparation . . . 17
3.7 Pervaporation module . . . 17
3.8 Fourier transform infrared spectroscopy . . . 19
3.9 Thermogravimetric analysis . . . 20

Results and discussion **21**
4.1 Contact angle measurements . . . 21
4.2 FTIR measurements . . . 22
4.3 Sorbtion tests . . . 23

4.4 Membrane morphology 24
4.5 Gas chromatograph 25
4.6 Thermogravimetric analysis 26
4.7 Pervaporation 27
4.7.1 The effect of feed composition 27

Conclusion **32**

Appendix **i**
A Risk assessment i
B Pervaporation results iii
C Results from gas chromatograph vii

Introduction

1.1 Motivation

Natural gas is one of the fastest growing energy sources in the world and will most likely continue to be used as energy for many decades still, and it is also the cleanest burning fossil fuel[2]. Most natural gas requires dehydration because most gas deposits contains water and this water can cause corrosion in the pipelines and hydrates to form. This dehydration is most commonly done with an absorption desorption process utilizing a glycol solution to absorb the water by flowing countercurrent to the gas flow in a large tower and then desorbing the water again by applying heat to the glycol-water solution in a reboiler[3]. This process is however not applicable to subsea operation and the subsea gas extraction therefore utilize additives that hinders the formation of hydrates and condensation in the tube while transporting the gas to the surface where it can be dehydrated. This is done because the absorption desorption process is not modular enough and requires too much maintenance to apply on the seafloor[1]. The towers required is also difficult to place on the seafloor so that it is not affected by the sea currents.

Membranes are currently being used in natural gas processing, however it is mostly only used for the removal of CO_2[4]. Membrane processes has many desirable advantages over the absorption-desorbtion processes. A membrane process is generally more compact than the absorption-desorption process since the absorption towers needs to be large to have a large enough contact area between the absorption solution and the gas. This is not a problem with the membrane process since the contact surface is the membrane surface and the membranes can be formed into for instance spiral-wound or hollow-fiber modules which are quite effective at increasing the surface area to volume ratio[5], which in turn reduces the footprint of the module drastically compared to the absorption towers. A membrane process can also reduce the energy cost of the operation because the regeneration of the absorption-liquid does not require a reboiler since a membrane can be used for this process as well. The ability to make the membrane process highly modular also helps with the maintenance and the installation on the seafloor[1].

A membrane dehydration process has therefore been proposed by SUBPRO a center for innovation based research within subsea production and processing at the Norwegian University of Science and Technology. The process consists of a membrane contactor and a membrane pervaporator where the contactor is in contact with the natural gas from the natural gas deposit on the feed side and a glycol solution on the permeate side and the pervaporation membrane is in contact with the glycol solution on the feed side and a sweep gas or vacuum on the permeate side. The contactor is as a replacement of the absorption tower while the pervaporation membrane is a replacement for the reboiler to regenerate the glycol solution. This thesis focuses on the pervaporation membrane and the dehydration of the glycol solution by pervaporation[1].

1.1.1 Research objectives

This project is part of a SUBPRO (Subsea production and processing) project. SUBPRO is a center for innovation-based research within subsea production and processing. The aim of this project is to investigate if a Polybenzimidazole (PBI) membrane is suitable for a pervaporation process for dehydrating triethylene glycol (TEG).

There has been done little research on the dehydration of TEG with the use of membrane pervaporation. Some research has been done previously with Teflon AF2400 as a part of the same research project at SUBPRO by Natalie Josefsen [6].

The goal of this project is to create and test a PBI membrane and testing the separation performance of this membrane when used in a pervaporation process with water and TEG at the feed side. Figure 1.1.1 shows the molecular structure of PBI.

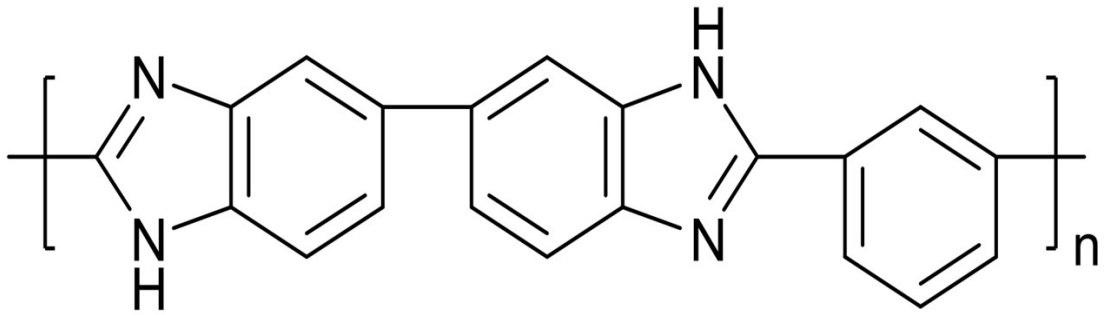

Figure 1.1.1: The molecular structure of polybenzimidazole.

Theory

2.1 Natural gas dehydration.

The most energy-efficient fossil fuel in use today is natural gas. It is also used as an important source for hydrocarbons for the petrochemical industry and elemental sulfur[2]. Natural gas deposits generally contain impurities like H_2S, CO_2 and water vapour[7]. There are many problems that can arise due to these impurities like corrosion and erosion of the pipeline and formation of solid hydrates and these impurities therefore needs to be removed from the gas stream before it enters the pipelines.

The most common methods for dehydration of natural gas used today are liquid and solid desiccant dehydration and cooling. The liquid desiccant dehydration utilizes the mass transfer of water into a liquid solvent, usually a glycol solution, and the solid desiccant dehydration utilizes the mass transfer of water into porous crystalline structures. The dehydration by cooling lowers the temperature of the gas below the dew point of the water causing the water to condense into a liquid. The most common of these three is the dehydration by liquid desiccant and is the method that is considered further in this project since it has the most similarities with the proposed membrane process[2].

In dehydration processes it is common to use a glycol solution to absorb the water. The different glycol solutions that are used is monoethylene glycol, diethylene glycol, triethylene glycol and tetraethylene glycol.[8]. Triethylene Glycol is the most commonly used desiccant for liquid dessicant dehydration due to its high theoretical decomposition temperature, $206°C$, its low vaporization loss, because it is easier to regenerate to $98 - 99\%$ and because it is cheaper than tetraethylene glycol which theoretically would be a better choise[8].

Dehydration with a triethylene glycol solution is most commonly done with an absorbtion-desorbtion process where the wet gas enters a glycol contactor at the bottom and the pure liquid TEG enters the contactor from the top. The TEG will then come into contact with the gas in a countercurrent and absorb the water and

the dehydrated gas can exit the top of the contactor. The TEG-water solution will then be sent to a reboiler where the solution is heated enough to release the water. This dehydrated TEG is then sent back to the top of the contactor to absorb more water.[8] A general flowchart of this process is included in figure 2.1.1.

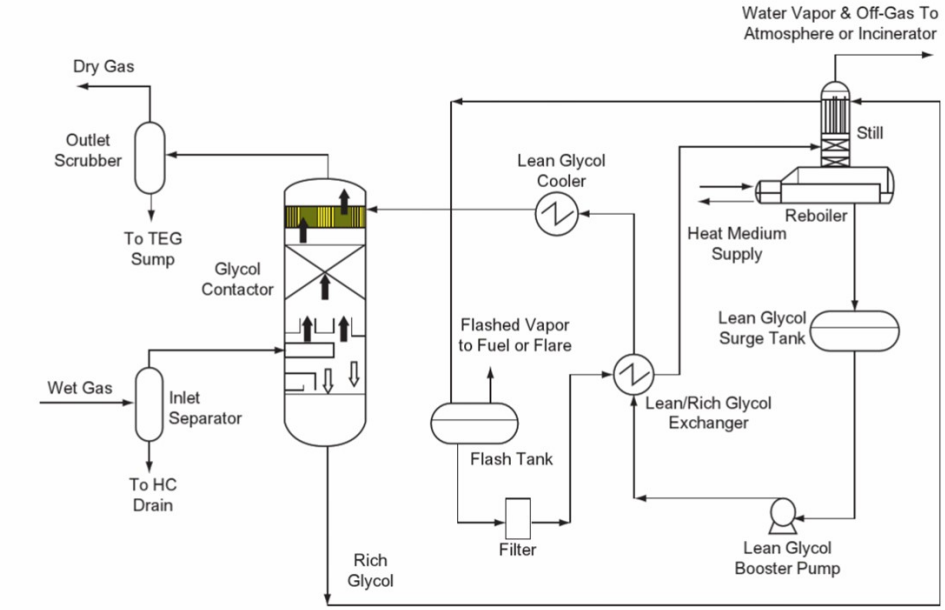

Figure 2.1.1: General flowchart of a TEG natural gas dehydration process found in Handbook of natural gas transmission and processing[8].

Even though this process is the process that is mostly used in dehydration of natural gas there are some disadvantages to this method. The problems includes insufficient dehydration, foaming and hydrocarbon solubillity in glycol. The reboiler also requires a large amount of energy to generate a sufficient amount of heat to make the glycol release the water[8].

2.2 Subsea natural gas processing

Subsea natural gas processing has recently been receiving a great deal of interest because potential oil and gas deposits are located under the sea in more remote places and in places where atmospheric conditions makes an offshore platform less viable to use for the production of these deposits. By moving the processing steps down to the seafloor the capital and operational costs can be lowered by a significant amount due to the common practice of adding chemicals to avoid the corrosion, errosion and hydrate problems when having the processing stages on a platform on the water surface[1]. The absorbtion-desorbtion method outlined in

section 2.1 is not a viable process to implement as a subsea dehydration method due to low modularity which presents a weight problem for the equipment used when installing it at the seafloor and due to the high maintenance requirements[1]. To solve these problems a membrane dehydration process has been proposed.

2.3 Membrane dehydration

A membrane process is a process where a polymer or a crystalline solid is used as a barrier separating different components in a gas-gas, liquid-gas or liquid-liquid solution. The mechanisms of transport in the polymeric membranes are generally based on the solution-diffusion model. When talking about the transport in a membrane two parameters are important, the permeability (P) and the selectivity (α). The permeability is the product of the solubility coefficient (S_i) and the diffusion coefficient (D_i) while the selectivity is the ratio of the permeability of the different permeants[9]. The selectivity is a measure of how good the separation of the different components are. When designing a membrane for subsea application a large problem is the loss of methane through the membrane and a high selectivity is therefore vital[1].

The membrane process suggested by SUBPRO is a combination of a membrane contactor and a membrane pervaporator. The contactor is in contact with the natural gas on the feed side and absorbs the water through a membrane into TEG on the permeate side. The pervaporation membrane is in contact with the TEG-water solution on the feed side and dehydrates the TEG-water solution[1]. A flowchart of the process is included in figure 2.3.1

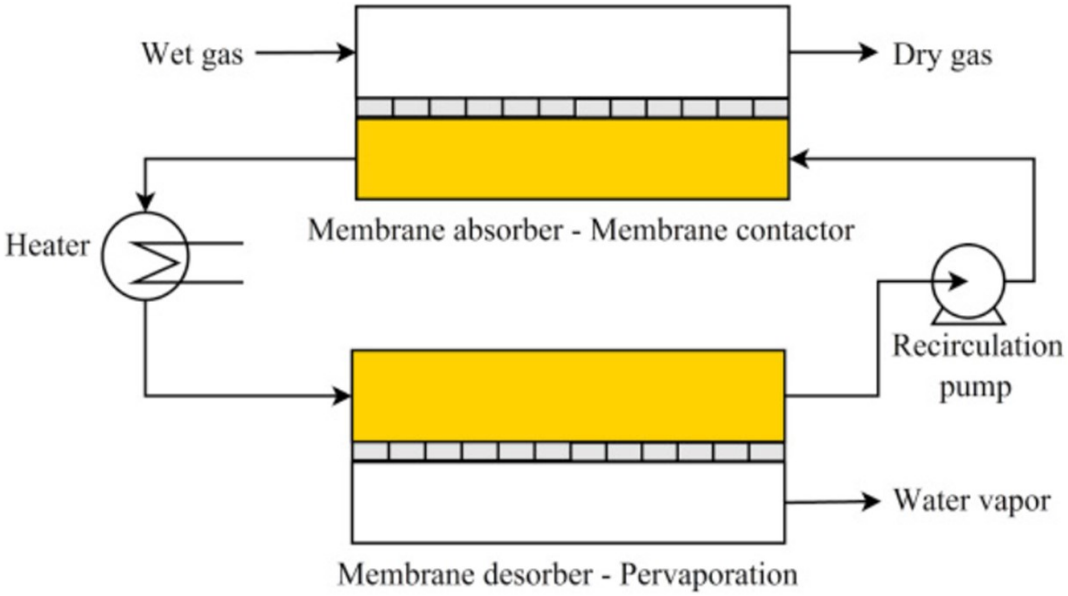

Figure 2.3.1: Figure showing the suggested membrane separation process found in Journal of Natural gas science and engineering[1].

The focus of this project is the dehydration of the TEG-water solution by the use of pervaporation to dehydrate TEG and the contactor is therefore not considered further.

2.4 Membrane pervaporation

Membrane pervaporation is a process that is used for liquid-liquid separation which utilizes a dense membrane for the separation. The driving force of the separation is the difference in the partial pressure (vapour pressure) of the components in the liquid solution and the vacuum or sweep gas that is applied at the permeate side of the membrane. This is a good way to select for the compounds that has the lower concentration since these components generally are more volatile than the other components which again means that the heat of the liquid mixture on the feed side has a large impact on the permeation rate of the compounds since a higher temperature leads to a higher vapour pressure. The transport is generally following the solution-diffusion model[10][11].

2.5 Membrane materials and membrane types for pervaporation

When choosing a membrane material for a pervaporation process there are many factors to consider. To avoid heavy maintenance the membrane needs to be both mechanically and chemically stable to ensure a long-term stability and a high performance. Most pervaporation processes are also performed at high temperatures and a high thermal stability will therefore be important as well[11].

Membranes can be made from different materials and are in general categorized into polymeric, inorganic and hybrid membranes. The most common membranes are in the polymeric category because the membranes are easier to manufacture, easier to scale up and relatively cost effective compared to the inorganic and hybrid membranes. There are however some drawbacks with a polymeric membrane compared to the other types of membrane. The polymeric membranes generally has a lower permeability and separation capabilities and a lower thermal and chemical resistance. The inorganic membranes generally has an excellent permeability and selectivity because the pores can be very uniform in size. The inorganic membranes however have problems with mechanical strength due to the crystalline structures and are highly difficult to manufacture meaning that the cost of these membranes is high. The hybrid membranes is a way to compromise between the polymeric membranes and the inorganic membranes by combining the high separation performance of the inorganic membranes with the easier manufacturing of the polymeric membranes. The hybrid membranes is created by introducing inorganic particles to a polymer during manufacturing. This however creates some compatibility issues between the inorganic and polymeric phases which has the possibility to decrease the separation capabilities drastically[11].

A polymeric membrane can be isotropic or a composite membrane. The isotropic membranes are prepared by solvent evaporation, which means that the polymer is dissolved in a solvent and poured onto a glass plate which followed by a slow evaporation of the solvent. This method gives a thick membrane in order for the membrane to be mechanically stable, which means that the separation performance is decreased. Due to this fact composite membranes are most often used in the industry. The composite membrane is a membrane which consists of a porous support coated with a thin film of a dense membrane. The thin film is the selective layer which determines the separation characteristics of the membrane while the porous support gives the mechanical strength. Since the thickness of the selective membrane affects the rate of permeation while keeping the selectivity of the membrane relatively constant the membrane performance of these membranes are generally higher than the isotropic membranes[11].

2.5.1 Solution-Diffusion model

There are two models commonly used to describe the mechanism of permeation in a membrane separation process. One is the pore-flow model and the other is the solution-diffusion model. The pore-flow model describes the permeation as a Knudsen diffusion or a molecular sieve through small pores in the membrane driven by a pressure gradient and the separation occurs because one or more of the permeants are excluded from the pores while other permeants can enter the pores. The difference between Knudsen diffusion and molecular sieve is that with Knudsen diffusion all of the molecules are large enough to enter the pores and the pores are narrow enough for the mean free path is higher than the diameter of the pore while in the molecular sieve model the pores are small enough to exclude one of the permeants which means that the selectivity depends on the size of the molecules[12]. In the solution-diffusion model the permeants are dissolved in the membrane followed by a diffusion through the membrane. The permeants are here separated by the differences in the solubility of the different permeants in the membrane as well as differences in the diffusion rates through the membrane. The pore-flow model is quite useful to describe the transport through a membrane with pores as small as around 5Å but breaks down with smaller pores[13].

The permeability of a species in the solution diffusion model can mathematically be described as the product of the solubility and the diffusion and is given in equation 2.5.1[14].

$$P = S \cdot D \tag{2.5.1}$$

Where P is the permeability ($[10^{-10}\frac{cm^3(STP)cm}{cm^2scmHg}]$), S is the solubility ($[\frac{cm^3(STP)}{cm^3cmHg}]$) and D is the Difusivity ($[\frac{cm^2}{s}]$). The permeability is most commonly measured in Barrer which is the unit given above. Fick's law is used to connect the permeability to the flux through the equation 2.5.2[14].

$$J_i = \frac{P_i A \Delta p}{l} \tag{2.5.2}$$

Where J_i is the molar flux of component i in $[\frac{mol}{s}]$, Δp is the difference in pressure over the membrane, A is the area of the membrane, l is the thickness of the membrane and P_i is the permeability of component i. When determining the selectivity of the membrane there are two different values that is useful to consider, the ideal selectivity and the actual selectivitywhich is more generally called the separation factor. The ideal selectivity is the ratio of the permeability of component i and j given in equation 2.5.3[14].

$$\alpha_{i,j} = \frac{P_i}{P_j} = \frac{D_i \cdot S_i}{D_j \cdot S_j} \tag{2.5.3}$$

Since the diffusion coefficients D_i and D_j is a measure of the mobility coefficients of the permeants in the membrane the ratio $\frac{D_i}{D_j}$ is a measure of the mobility selectivity of the membrane and can be seen as reflecting the difference in size of the permeants. A larger permeant size will give a lower diffusion coefficient. The ratio o the solubility coefficients, $\frac{S_i}{S_j}$, on the other hand can be seen as the solubility selectivity which shows the difference in the condensability of the different permeants. Since the condensability of a molecule generaly increases with molecular size the solubility selectivity usually shows the opposite trend than the mobility selectivity[15]. The separation factor is the ratio of the fraction of the permeants on the feed side over the fraction of the permeants on the permeate side of the membrane and is given in equation 2.5.4.

$$\alpha^*_{i,j} = \frac{\frac{y_i}{y_j}}{\frac{x_i}{x_j}} \tag{2.5.4}$$

Where x_i and x_j refers to the mole fraction of component i and j on the feed side and y_i and y_j refers to the mole fractions on the permeate side. The separation factor will be the same as the ideal selectivity at standard temperature and pressure, but since the separation factor is dependent on the operation conditions the values will not be the same at different temperatures and pressures[15].

2.5.2 Free volume theory

The free-volume theory is a quantitative description of the diffusion coefficients concentration dependence, and is based on the observation that the diffusion through a polymer is generally much higher when the polymer is in its rubbery state than in its glassy state[16].

When the polymer is below the glass transition temperature, (in its glassy state), the polymer chains lacks the thermal energy to allow rotation around the main chain and the movement is largely limited to the side-groups. In the rubbery state however the thermal energy is high enough to allow for movement around the main chain. This freedom of movement will therefore create more microvoids inside the polymer which will allow for a larger rate of diffusion[16].

The free volume, V_f, of a polymer can be defined as the volume generated by thermal expansion of the polymer at an initial state at $0°K$[16].

$$V_f = V_T - V_0 \tag{2.5.5}$$

Where V_T is the volume at temperature T and V_0 is the volume at $0°K$. The fractional free volume v_f is then defined as[16].

$$v_f = \frac{V_f}{V_T} \tag{2.5.6}$$

The basic concept of the free-volume diffusion is that a molecule can only move from one place to another if there is sufficient empty space. This means that if the size of the penetrant increases the free volume of the polymer needs to increase to allow for the diffusion of the penetrant[16].

2.5.3 Membrane pervaporation theory

In pervaporation one of the interfaces of the membrane is in contact with a liquid feed fluid at a higher pressure than the saturation vapour pressure while the other membrane interface is under a continuous vacuum. This results in a selective separation of the component with the lowest concentration from the feed. Since the chemical potential at the liquid/membrane interface is in equilibrium with the chemical potential inside the membrane the equation for the chemical potential becomes[13].

$$\mu_i^\circ + RTln(\gamma_{i0}^L \chi_{i_0}) + \nu_i(p_0 - p_{i_{sat}}) = \mu_i^\circ + RTln(\gamma_{i_{0(m)}} \chi_{i_{0(m)}}) + \nu_i(p_0 - p_{i_{sat}}) \tag{2.5.7}$$

Where the L pertains to the liquid solution, the subscript m pertains to the membrane, R is the ideal gas constant, T is the temperature, μ_i° is the reference chemical potential of pure component i at a reference pressure p_i°,γ_{i_0} is the activity coefficient of component i, $_i$ is the mole fraction of component i and ν_i is the molar volume of component i. When rearranging this equation you can get an equation for the concentration[13].

$$c_{i_{0(m)}} = \frac{\gamma_{i,0}\rho_m}{\gamma_{i_{o(m)}}\rho_0} c_{i_0} = S_i^L c_{i_0} \tag{2.5.8}$$

Where S_i^L is the liquid phase sorption coefficient $\frac{\gamma_{i,0}\rho_m}{\gamma_{i_{o(m)}}\rho_0}$. At the permeate side of the membrane the pressure will drop from p_0 at the membrane interface, to p_l in the permeate gas phase. This gives an equation for the chemical potential[13].

$$\mu_i^\circ + RTln(\gamma_{i_l}^G \chi_{i_0}) + RTln\left(\frac{p_l}{p_{i_{sat}}}\right) = \mu_i^\circ + RTln(\gamma_{i_{l(m)}} \chi_{i_{l(m)}}) + \nu_i(p_0 - p_{i_{sat}}) \quad (2.5.9)$$

Which can be rearranged to

$$\chi_{i_{l(m)}} = \frac{\gamma_{i_l}^G}{\gamma_{i_{l(m)}}} \frac{p_l}{p_{i_{sat}}} \chi_{i_l} e^{\left(\frac{-\nu_i\left(p_0 - p_{i_{sat}}\right)}{RT}\right)} \quad (2.5.10)$$

The exponential term, known as the Poynting correction factor, can generally be neglected because it is usually equal to one or close to one. By assuming that the poynting factor is equal to one the equation becomes[13].

$$\chi_{i_{l(m)}} = \frac{\gamma_{i_l}^G}{\gamma_{i_{l(m)}}} \frac{p_{i_l}}{p_{i_{sat}}} \quad (2.5.11)$$

Introducing the consentration $c_{i_{l(m)}}$ the equation can be written as[13].

$$c_{i_{l(m)}} = m_i \rho_m \frac{\gamma_{i_l}^G p_{i_l}}{\gamma_{i_{l(m)}} p_{i_{sat}}} = S_i^G p_{i_l} \quad (2.5.12)$$

By combining Fick's law, 2.5.8 and 2.5.12 the permeation flux of the membrane can be expressed as[13].

$$J_i = D_i \frac{\left(S_i^L c_{i_0} - S_i^G p_{i_l}\right)}{l} \quad (2.5.13)$$

This equation contains two different sorption coefficients, S_i^L and S_i^G, where S_i^L is for the liquid phase and S_i^G is for the gas phase. By considering a hypothetical vapor-liquid equilibrium[13].

$$\mu_{i_0} + RTln\left(\gamma_i^L \chi_i^L\right) + \nu_i\left(p - p_{i_{sat}}\right) = \mu_{i_0} + RTln\left(\gamma_i^G \chi_i^G\right) + RTln\left(\frac{p_0}{p_{i_{sat}}}\right) \quad (2.5.14)$$

And then introducing the concentration c_i^L this equation can be rewritten as.

$$c_i^L = \left(\frac{S_i^G}{S_i^L}\right) p_i \quad (2.5.15)$$

By substituting equation 2.5.15 into equation 2.5.13 and defining $D_i S_i$ as the permeability P_i the equation becomes

$$J_i = \frac{P_i \Delta p}{l} \tag{2.5.16}$$

By introducing a liquid feed Δp can be defined as $(x_i \gamma_i p_i^0 - y_i p_p)$ where x_i and y_i is the mole fraction of component i in the feed and the permeate respectively, p_i^0 is the saturation pressure of pure i at the given temperature, p_p is the pressure at the permeate side and γ_i is the activity coefficient of i. The saturation pressure p_i^0 can be determined by the Antoine equation[13].

$$log(p) = A - \frac{B}{C - T} \tag{2.5.17}$$

Where A, B and C are constants that are specific to the species and can be found in literature.

The temperature dependence of the permeability is often described by the Arrhenius relation

$$P_i = P_0 e^{-\frac{E_J}{RT}} \tag{2.5.18}$$

Where P_0 is a preexponential factor of permeance and E_J is the apparent activation energy of the permeance. [17]

Experimental

3.1 Membrane materials

The material used for the membrane in this study was Celazole® S26 polybenzimidazole solution which contains 26% solid polybenzimidazole and was purchased from PBI Performance Products, Inc. This solution was diluted in N,N-Dimethylacetamide, Anhydrous 99.8% purchased from Sigma Aldrich. The support was microporous polypropylene Celgard 2400 supplied by Celgard Company with a thickness of $25\mu m$ and a porosity of 41%.

3.2 Membrane preparation

The membrane was prepared by diluting the polybenzimidazole S26 solution to $15wt\%$ solution in $DMAc$. The solution was stirred for 24 hours until a homogenous solution was obtained. The solution was then cast on a porous polypropylene support using a casting knife with an initial gap of $80\mu m$. The composite membrane were placed in an oven overnight at $80°C$ under continuous vacuum. The dried membrane was then immersed in deionized water for 48 hours to remove all $LiCl$ from the polymer matrix. The water was changed every day. The composite membrane was then heated up to $80°C$ under vacuum for 24 hours to remove the water and residual solvents from the membrane. It should be noted that the melting temperature of the polypropylene support is approximately $120°C$.The dried membrane was then characterized by SEM and tested in a pervaporation setup. To check the TEG sorption and to perform compatibility tests, a free standing polybenzimidazole membrane was prepared from a 15% PBI solution. The drying protocol was modified since the support was not utilized. The washed self-standing membrane was dried up to $190°C$ to remove all the water and residual solvents.

3.3 Contact angle measurements

To determine the breakthrough pressure of water and TEG in porous polypropylene the Young-Laplace equation was used. The equation requires the surface

tension σ of the liquid, the contact angle θ between the liquid and the membrane and the pore size r of the membrane pores.

$$\Delta p = -\frac{2\sigma cos\theta}{r} \tag{3.3.1}$$

The surface tension of the liquids can be found in the literature and the contact angle was measured with an Attension optical tensiometer. This method was also utilized on PBI to determine its affinity towards water and TEG.

An optical tensiometer is a camera that is pointing perpendicular to the surface of the material that is to be studied. A drop of the liquid that the contact angle is to be measured is then placed on the material and the angle on both sides of the droplet is then measured and the average is then the contact angle of that liquid on the material.

3.4 TEG sorbtion tests

To determine if the PBI layer on the membrane is absorbing TEG, pieces of the pure PBI membrane were weighed and then submerged in pure TEG. The pieces were cleaned and then weighed again after 2, 4, 6, 24, 48 and 168 hours. For each time increment three different pieces were weighed after removing as much of the liquid on the surface as possible.

3.5 Membrane morphology

To determine the morphology of the membrane a scanning electron microscope (SEM) was used. The SEM used was a Hitachi TM3030 Plus and the samples were coated with a $5nm$ thick gold layer by a sputter coater, Quorum Q150R, to make them conductive.

The samples were prepared by freeze fracturing the membrane by first absorbing ethanol followed by a liquid nitrogen bath to make the membrane as brittle as possible. The membrane sample were then attached to a sample holder with conductive tape and coated with a $5nm$ gold layer and then placed inside the SEM for study.

3.6 Gas chromatography

Gas chromatography is a process where the chemical constituents of a sample is separated by their interactions with an inert carrier gas commonly called the mobile phase and a liquid or solid coating inside the capillary column. The capillary column is a thin long tube and together with the stationary phase and the mobile

phase separates the sample due to the fact that the different molecules has a different residence time inside the column. Meaning the different molecules are slowed down by a different amount due to the interactions with both the wall of the column and with the stationary phase. To make the separation possible the sample needs to be vaporized so that it can travel with the mobile phase through the column. This separation means that the different constituents of the sample can be registered separately at the outlet of the capillary column. The registration of the different components of the sample can be done with multiple different detectors like thermal conductivity (TCD), flame ionization (FID), nitrogen-phosphorous (NPD), flame photometric (FPD), electron capture (ECD) and by mass spectrometry. Regardles of which detection method is utilized the detector generates a signal separated in time where each peak is related to the quantity of a single component, an example of such a signal is given in figure 3.6.1[18].

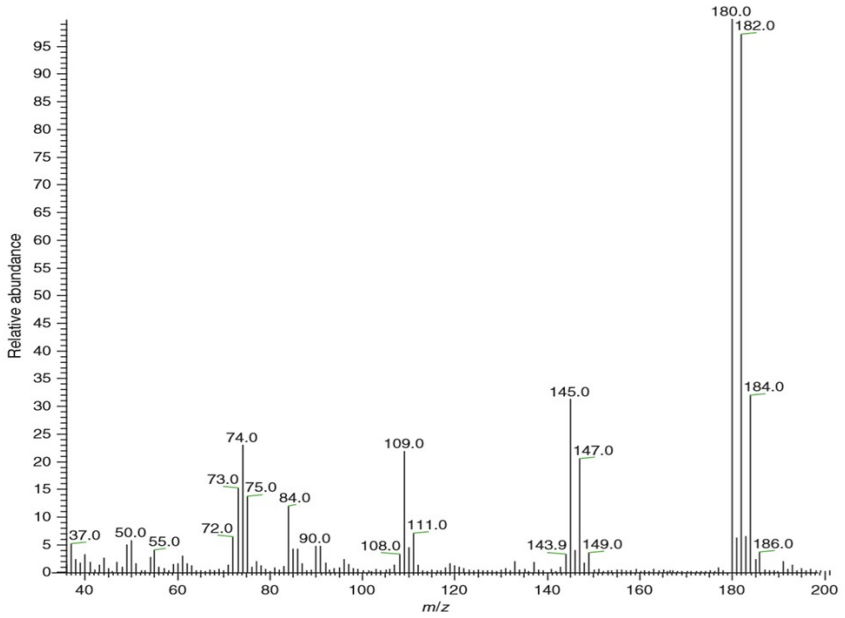

Figure 3.6.1: Example of a signal from a gas chromatograph

To be able to interpret the results from the gas chromatography a baseline needs to be established. This is usually done by establishing a base curve where a range of known concentrations of the compound that is to be detected is tested. The peaks of the signals can then be related to the concentrations to establish the base curve which the samples will later be compared to. In addition to this calibration curve an internal standard is often used. The internal standard is a solution of a compound with a chemical similarity to the compound that is to be measured. The

internal standard can then be added to every sample with a known concentration to establish a reference.

The gas chromatograph used in this project was an Agilent Technologies 7820A GC system. The calibration curve for this experiment was made by preparing samples with known concentrations of TEG between $10PPM$ and $500PPM$. These solutions were then tested in the gas chromatograph and the calibration curve was fitted to the peaks of the resulting spectra. A sample with $1wt\%$ Triethylene glycol monoethyl ether ($TEGME$) was prepared and $100\mu L$ of this solution was added to $900\mu L$ of deionized water to create a $1000PPM$ internal standard solution.

3.6.1 Gas chromatography test preparation

The samples were prepared by mixing $1000\mu L$ of the permeate from the pervaporation setup with $100\mu L$ of the internal standard which was chosen to be $1000PPM$ $TEGME$. All of the samples were weighed and the mass concentration were used for both the calibration and tests. The internal standard were created by mixing $900\mu L$ of de-ionized water with $100\mu L$ of a $1wt\%$ solution of $TEGMEE$ in water. In the cases where the permeate from the pervaporation tests was less than $1000\mu L$ the sample was prepared by taking a lower amount of both the permeate and the internal standard while keeping the same ratio of $1:10$. For instance by taking $500\mu L$ from the permeate and $50\mu L$ from the $1000PPM$ internal standard.

3.7 Pervaporation module

The membranes were tested in a pervaporation setup where the membrane were placed inside a membrane module. The membrane was supported by a sintered plate with an effective surface area of $35{,}8cm^2$ with large enough pores to allow for a free flow of the permeate through the plate. The liquid TEG/water feed was kept in a liquid reservoir and circulated with a circulation pump. The liquid were pumped into a temperature controlled box and through two heating coils and into the membrane sampleholder on the feed side before it went back into the liquid reservoir. The permeate side utilized a vacuum pump to create a pressure difference between the feed and permeate side of the membrane. The permeate was collected in a sampleholder that was cooled by liquid nitrogen to ensure condensation and a liquid nitrogen trap was also placed in front of the vacuum pump to avoid vapour from entering the pump. Since the membrane module was located inside the heating cabinet the flow rate was set to be quite low, $0{,}308\frac{ml}{s}$, to keep the temperature at a constant value over the membrane surface. The feed solution was changed between each temperature since over a longterm operation of the module the feed concentration would change due to the small size of the liquid reservoir.

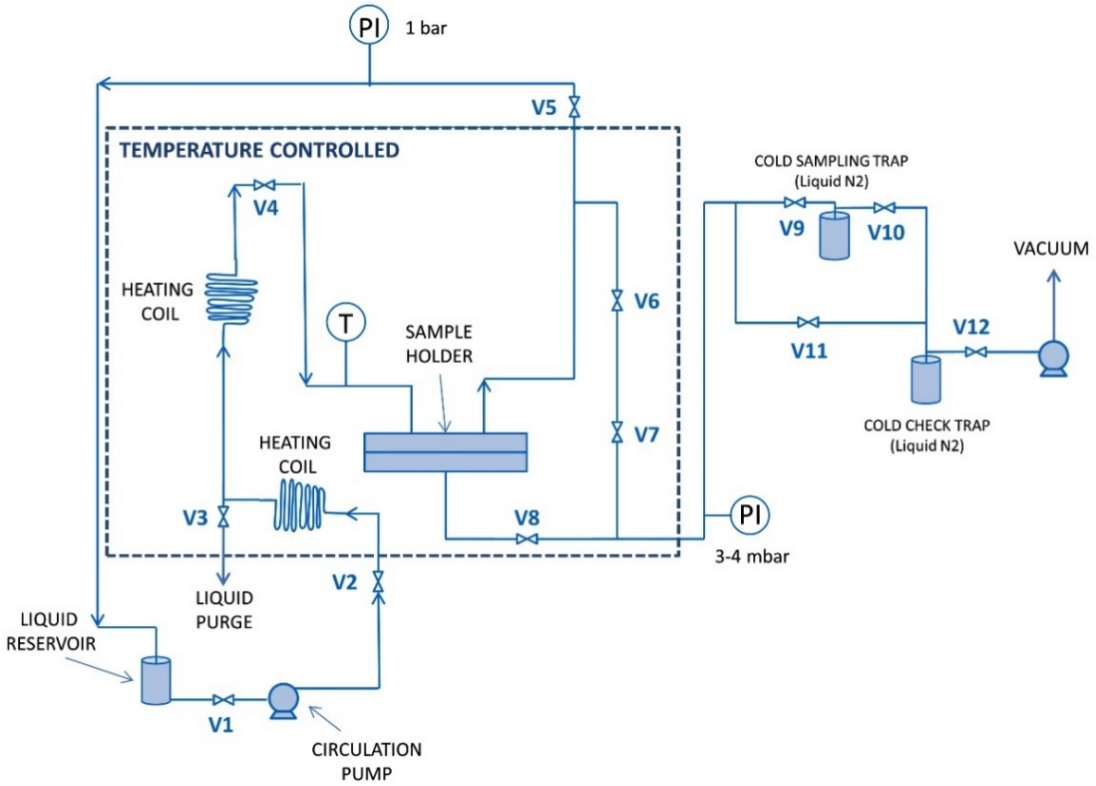

Figure 3.7.1: Flowchart of the pervaporation setup.

The sampleholders were put under vacuum and weighed before the test and weighed again after the test. This weight was then used to determine the flux from the equation

$$J_i = \frac{Q_a - Q_b}{At} \tag{3.7.1}$$

Where Q_a is the total mass of the sampleholder after the test, Q_b is the total mass of the sampleholder before the test, A is the area of the membrane and t is the time.

These tests were performed with a membrane of PBI on a support of polypropylene first with pure water in the feed, and later with $10wt\%$, $20wt\%$ and $30wt\%$ of water in a TEG solution at temperatures of $30 - 80°C$

3.8 Fourier transform infrared spectroscopy

Fourier transform infrared spectroscopy (FTIR) is a spectroscopy method that uses a signal from an interferometer. An interferometer is an instrument that splits a beam and merging them again do create different patterns of interference due to the phase difference of the beams due to different travel lengths. A simple Michelson interferometer is illustrated in figure 3.8.1.

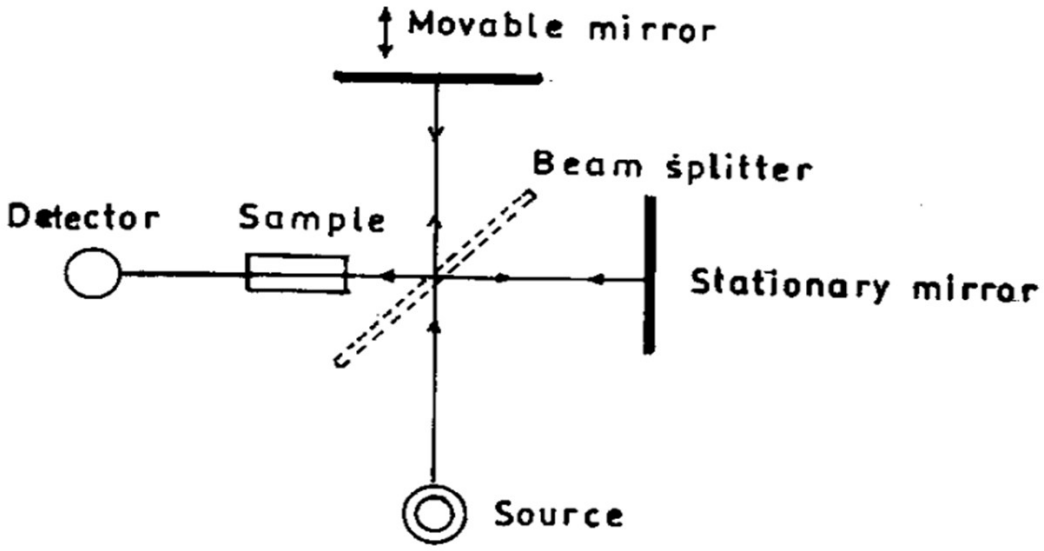

Figure 3.8.1: A simple diagram of a Michelson interferometer.

Fourier transform can then be used to generate a spectrum corresponding to the frequency of the signal by the fourier transform equations 3.8.1 and 3.8.2, which is the inverse fourier transform and the fourier transform respectively.

$$S(\nu) = \int_{-\infty}^{\infty} I(x) e^{+i2\pi\nu x} dx = F^{-1}[I(x)] \tag{3.8.1}$$

$$I(x) = \int_{-\infty}^{\infty} e^{-i2\pi\nu x} d\nu = F[S(\nu)] \tag{3.8.2}$$

Where x is distance and ν is the frequency. If a sample is placed in the beam emanating from the interferometer the different molecular bonds in the molecules will absorb different wavelengths of light and an absorbtion spectrum can be created

which can be used as an indication of which molecular bonds are present in the sample.

The FTIR system used in this project was an Thermo Fisher Nicolet iS50 FT-IR and was used to determine if the water was completely removed from the PBI membrane after the casting and drying process described in section 3.2 by testing a piece of the membrane taken before and after the boiling and drying process. The results from these tests were compared to the results from Musto et al (2018)[19].

It was also used to determine the presence of water in the membrane in the compatibility test and to indicate if the concentration of TEG was within the limits for the gas chromatograph by creating spectra for pure water, 1000ppm TEG in water and 1% TEG in water and comparing the spectra from the samples.

3.9 Thermogravimetric analysis

Thermogravimetric analysis is an instrument that measures a samples weight continuously in a controlled atmosphere while heating or cooling the sample. This allows for measuring the weight-loss of the sample accurately at specific temperatures and measure the weight-loss as a function of temperature which is a good way to determine the purity of a sample and the decomposition temperatures[20].

The TGA used in this project is the Netsch TG 209 libra. The TGA was used in this project to determine if the LiCl and DMAc was completely removed from the selfstanding membrane by sampling the membrane before and after the boiling and washing process.

Results and discussion

4.1 Contact angle measurements

The contact angle of TEG and water on the PBI/PP membrane was measured by using a tensiometer to be approximately 36,7° and 74,30° respectively. The contact angles for water and TEG on pure PP was also measured to be 115° and 89.41° respectively. This means that the PBI has a higher affinity to TEG than water while the PP has a higher affinity towards water than to TEG.

While the breakthrough pressure might not be applicable to a dense membrane due to the fact that the solution-diffusion model does not utilize pores in the membrane, it can be utilized when discussing the permeability of the porous support. Using the Young-Laplace equation (equation 3.3.1) together with the surface tension, the contact angle and the diameter of the pores the breakthrough pressure was calculated. The contact angle for pure water was found to be 115,96° and with a surface tension of $71{,}1\frac{mN}{m}$ and a pore diameter of $0{,}2\mu m$ the breakthrough pressure was calculated to be $6{,}86bar$. The same calculations for TEG with a contact angle of 89,41° and a surface tension of $45{,}5\frac{mN}{m}$ gave a breakthrough pressure of $-0{,}57bar$. Since the breakthrough pressure of TEG in polypropylene was negative it is inevitable that the membrane would be wetted by TEG if there is no barrier between the membrane and the TEG. Due to this the polypropylene is not suitable for separating water from TEG in itself, but it can still be utilized as a mechanical support for a selective layer so that as long as the selective layer is selective enough the separation of the membrane will still be good. The polypropylene should however probably be changed to another polymer at a later date due to problems with the heat resistance of the polymer as well as if the selective layer is damaged so that the TEG-water solution is in direct contact with the polypropylene the TEG flux would probably increase significantly.

4.2 FTIR measurements

FTIR was used to determine if the membrane contains water. To determine this a sample of the membrane was taken before the boiling and soaking outlined in section 3.2 and after the membrane had been dried. The FTIR spectrums of these samples are given in figure 4.2.1.

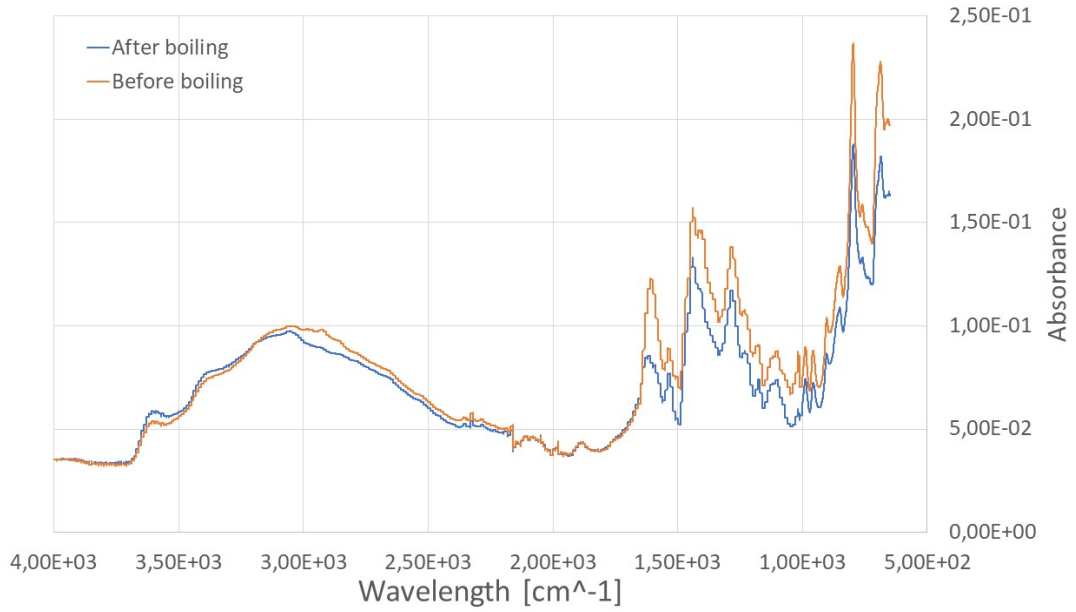

Figure 4.2.1: Graph of the FTIR absorbance spectrum of the PBI membrane before and after the boiling outlined in section 3.2

When comparing these FTIR spectra there is no discernible difference. Some of the peaks are different height, however this can be due to a difference in the ambient conditions at the time the tests were done. The important part is that the peaks are occuring in the same places which means that the samples are absorbing the same wavelengts of light and it can therefore be assumed that the samples has almost the same composition. These samples can be compared with the results from Musto et al[19] shown in figure 4.2.2.

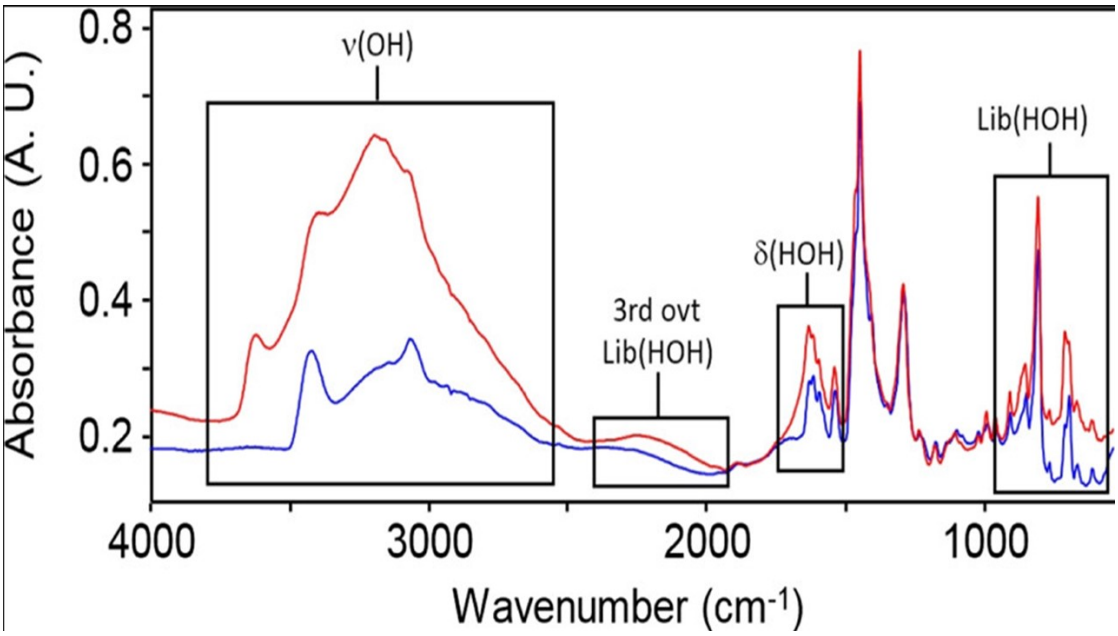

Figure 4.2.2: Figure showing an FTIR spectrum from a dry PBI membrane and a membrane with a high water content. The blue line is the dry PBI membrane and the red is the PBI membrane with a high water content. This graph can be found in a study by Musto et al[19].

When comparing the spectra in figure 4.2.1 and figure 4.2.2 there are some differences. The spectrums found in this experiment is more comparable to the membrane with a high water content from Musto et al than to the dried membrane which means that the drying stage was not sufficient to remove all the water from the selfstanding PBI membrane prepared in this project. To be able to remove all of the water a longer drying time should therefore be used in the future.

4.3 Sorbtion tests

To determine if PBI would absorb TEG and water pieces of PBI prepared as stated in section 3.2 was submerged in both a pure TEG solution and in a $20wt\%$ water-TEG solution. The pieces was weighed before the test and 3 pieces were weighed again after 2, 4, 6, 24, 48 and 168 hours. These tests showed a large uptake of TEG. The results were quite inconsistent however and previous studies has shown that the uptake of TEG in PBI is 0 and the results could possibly be attributed to either residual $LiCl$ or $DMAc$ in the membrane. Another membrane was therefore made where the membrane was not boiled and the soaking in pure water was done for 48 hours in stead of 24 hours. When testing the new membrane the TEG uptake was shown to be 0. The results from the second test is given in table 4.3.1.

Time [h]	Weight at time 0 [g]	Weight after test [g]
1	7.1	7.2
3	7.3	7.3
6	5.4	5.1
24	8.7	8.6
48	10.6	10.2
72	4.1	4.0
168	12.2	11.8

Table 4.3.1: Results of the sorbtion test with PBI in pure TEG

A previous study by Musto et al[19] also showed that the TEG uptake in PBI was minimal. The study also showed that PBI has a possibility to absorb water which in turn can change the separation performance of the membrane by increasing the size of the microvoids and allow for both more water and TEG to pass through the membrane. This might seem like a good characteristic since it will increase the amount of water that passes through the membrane, however since the amount of TEG that passes through will also increase and the permeability of TEG will probably increase by a larger amount than the permeability of the water since the PBI has a higher concentation on the feed side and it will therefore also decrease the selectivity of the membrane.

4.4 Membrane morphology

The thickness of the membrane was measured using a scanning electron microscope on the crossection of the membrane. The membrane was cut by soaking it in ethanol followed by a submersion in liquid nitrogen. This was done to cause as little disfiguration of the membrane as possible. The thickness of the selective PBI layer was determined to be at $2{,}5\mu m \pm 0{,}2\mu m$ as seen in figure 4.4.1. This was done because the flux through the membrane is dependant on the thickness of the membrane as seen in equation 2.5.16, so a thinner membrane will result in a higher flux through the membrane while not significantly impacting the separation performance, and it should therefore be done a similar study with a PBI membrane with a thinner dense layer to determine how much the permeation changes with the thickness of the PBI.

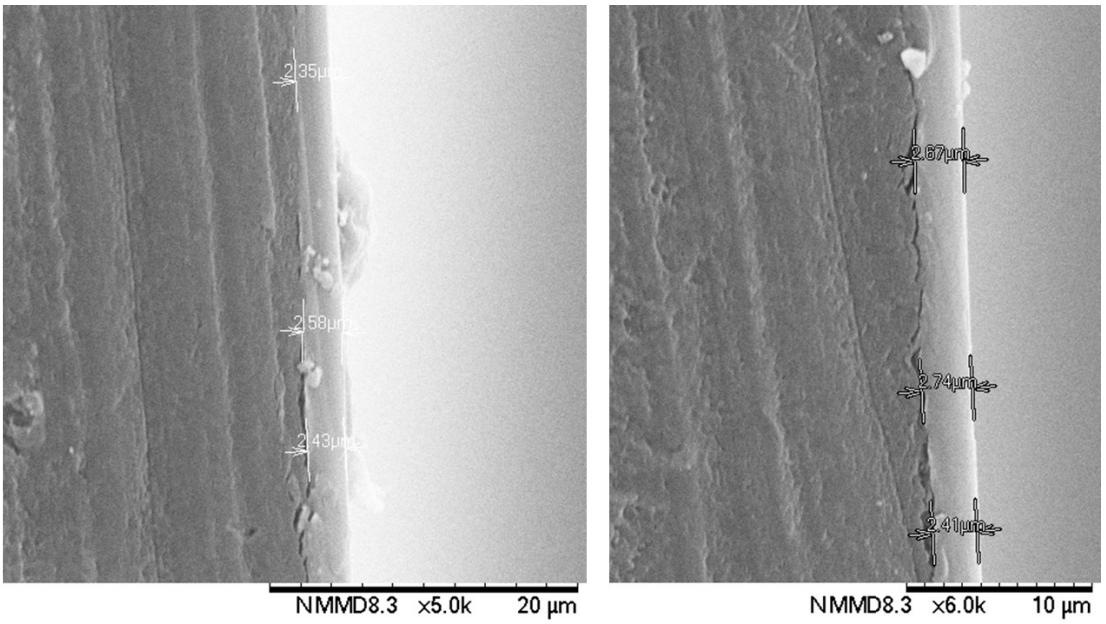

Figure 4.4.1: Two SEM pictures of the crossection of the PBI on PP membrane used in the pervaporation tests. The thickness was here measured with the SEMs own measurement tool.

The sample used for the SEM was taken from a small part of the membrane since it is not possible to test the entire membrane with this method without ruining the part of the membrane that is supposed to be used further in the pervaporation tests. It can however be used as an indication of the thickness and since the thickness was rather consistent over the sample it can then be assumed that this thickness is consistent over the entire membrane.

4.5 Gas chromatograph

The concentration of TEG in the permeate was determined with a gas chromatograph as stated in section 3.6. The results from the GC tests are given in table C.1. When plotting these results with respect to the feed temperature at different feed water content the predicted results should be strictly increasing due to the Arrhenius relationship given in equation 2.5.18. However this is not what the gas chromatography shows. The gas chromatography showed a large irregularity in the TEG concentration of the permeate and this could be caused by the way the permeation setup is designed, since the sintered plate gives a place for the TEG to condensate and therefore a place to gather up and then be released later in droplets which in turn could cause the concentration of TEG in the samples to be lower or higher than they should be. The same could also happen in the tubes

leading from the sintered plate to the sampleholder where the TEG could condensate on the walls of the tube and therefore cause a lower concentration in the sample the droplet really belonged to from while increasing the concentration in a later sample. Seeing as the concentration of TEG is so inconsistent after the gas chromatography tests it is not possible to say anything definite about the temperature dependence of the TEG permeation. All of the concentrations are however lower than $550PPM$ which is a low concentration and it can be said that the separation performance was quite good which can be seen as an indication that PBI is a suitable membrane material for the dehydration of TEG by pervaporation. The pervaporation setup should however be modified before another series of tests to avoid the gathering of TEG in the downstream pipes and the sintering plate. A solution could be to use an alternative cooling solution to gather the permeate since the current system with liquid nitrogen requires someone to continuously monitor the level of liquid nitrogen in the container and therefore limits the length of the experiments to a single day. This could contribute to a larger sample size and therefore a smaller error. The first thing to do however should be to find an alternative to the sintered plate and to possibly shortening the tubes between the membrane and the sampleholder.

4.6 Thermogravimetric analysis

The TGA curves of the selfstanding PBI membrane before and after boiling are plotted in figure 4.6.1. The TGA analysis was performed to understand the thermal behavior of the PBI and to determine if the LiCl and DMAc was removed in the preparation process. As it can be seen from the curves, the membrane before boiling (PBI-B-Boiling) shows a weight-loss in three distinct stages while two steps of weight loss was observed for the membrane after boiling (PBI-A-Boiling). The PBI-A-Boiling sample was boiled in deionized water and dried at 192 C overnight while the PBI-B-Boiling sample was taken before the boiling and drying stages. The PBI-B-Boiling sample shows a distinct drop in weight between $30°C$ to $165°C$ which is the boiling point of DMAc, while the PBI-A-Boiling sample maintains a constant weight in this temperature region. This is an indication that the PBI-A-Boiling membrane contains LiCl and a small amount of DMAc. The curve then remains stable up to around $550°C$. From $550°C$, the decomposition step of the polymer starts. The PBI-B-Boiling membrane shows the same weight loss trend as the PBI-A-Boiling membrane from $30°C$ to $165°C$. When comparing the PBI-B-Boiling curve to the PBI-A-Boiling curve, it is clear that the membrane before boiling has LiCl left in the polymer matrix. Above $500°C$, the decomposition step shows the same trend and weight loss. It can therefore be concluded that the LiCl and DMAc has been removed from the matrix in the boiled membrane which means that the preparation procedure results in a pure membrane.

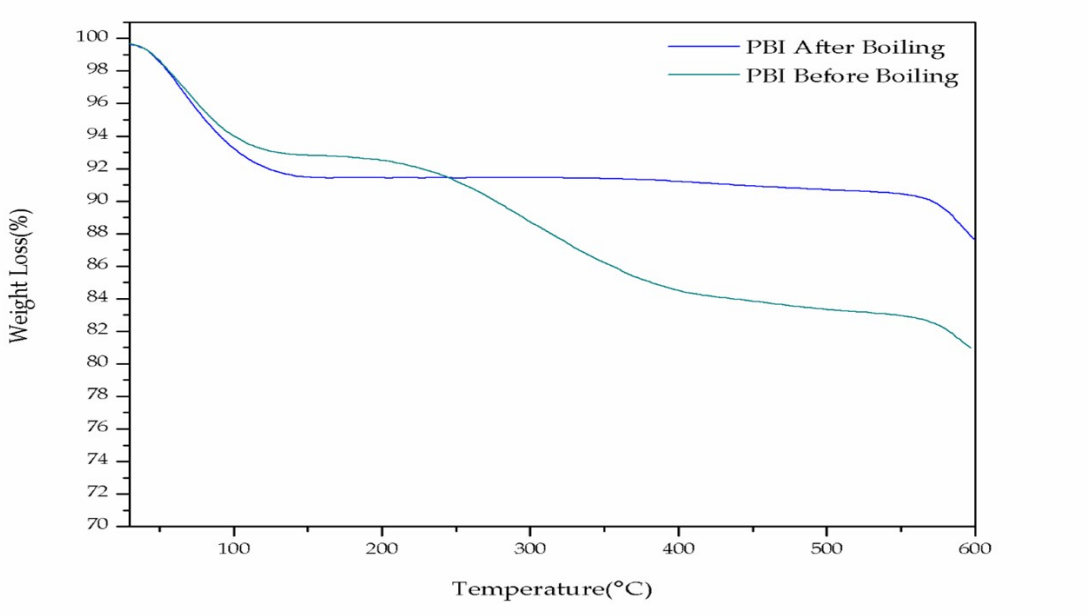

Figure 4.6.1: Thermogravimetric analysis of the selfstanding PBI membrane before and after boiling.

4.7 Pervaporation

The membrane was tested with pure water and a solution of $10wt\%$, $20wt\%$ and $30wt\%$ water in TEG on the feed side. This allows for a comparison of the effect this difference has on the permeate. These test were done at a temperature of 30, 40, 50, 60, 70 and $80°C$ with pure water in the feed and with $30wt\%$ water in TEG. The 30 and $40°C$ was skipped for the $20wt\%$ because the flux was too low to get a large enough sample for the gas chromatograph. These temperatures were not skipped for the $10wt\%$ samples since these tests were carried out first, but the sample size was here also too small for the gas chromatograph.

4.7.1 The effect of feed composition

The feed composition has a large effect on the total flux through the membrane as shown in figure 4.7.1. The trend is fairly linear at 30 and $40°C$ and at 50, 60, 70 and $80°C$ the flux increases at a higher rate with higher water feed concentration. At $30°C$ the flux does not change by a large amount, however as seen in 4.7.1 the feed composition has a larger effect when increasing the temperature. The measurements for $20wt\%$ at 30 and $40°C$ was not done, but it is reasonable to assume that the flux would follow the same trend as for 50, 60, 70 and $80°C$ where the flux increases by a larger amount from $20wt\%$ to $30wt\%$ than from $10wt\%$ to

$20wt\%$. From equation 2.5.16 and introducing the expression $(x_i\gamma_i p_i^0 - y_i p_p)$ for Δp it can be seen that the flux should have a linear relationship with respect to the driving force if the activity coefficient γ_i is constant. When looking at figure 4.7.1 it is clear that the activity coefficient has to be changing. When taking the Due to the hydrogen on the nitrogen atoms in the PBI matrix the PBI is able to form hydrogen bonds with the water molecules and therefore increase the solubility of water in the membrane. This can then cause the membrane to swell with water which will increase the free volume of the membrane which again will increase the flux of water through the membrane. The TEG flux will also increase when the free volume of the membrane increases, however the TEG molecules are significantly larger than the water molecules which in turn means that the water flux will increase more than the TEG flux. This effect will increase with the concentration of water since this will increase the swelling.

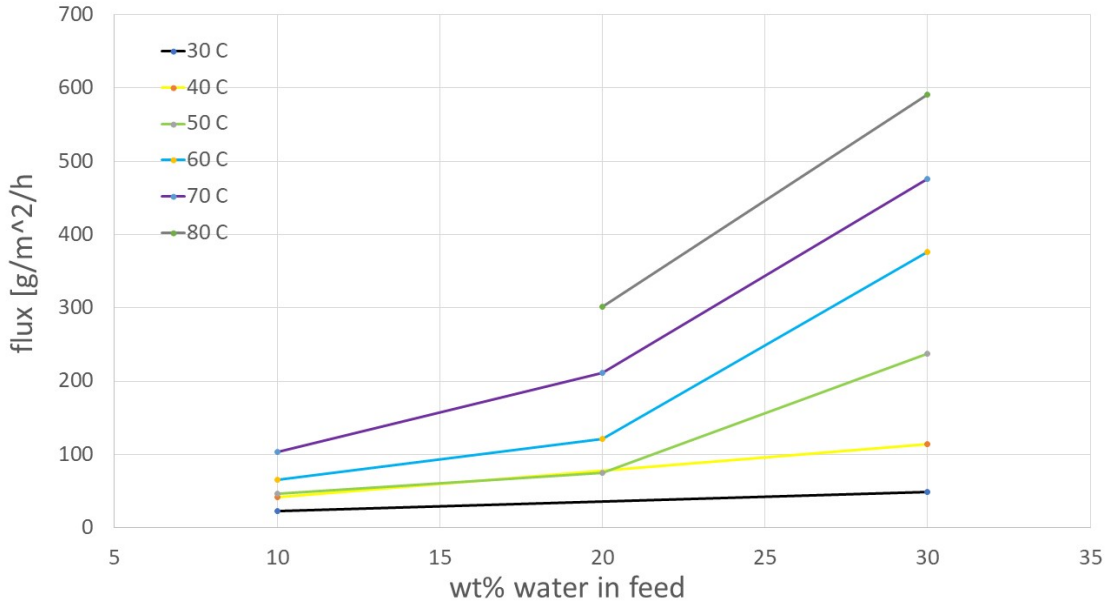

Figure 4.7.1: Graph showing the effect of feed composition on the total flux at different temperatures.

The permeate from the membrane was tested with a gas chromatograph to determine the amount of TEG that permeated the membrane. The concentration was measured in PPM, parts per million, and is given in figure 4.7.2. In this figure it can be seen that there is no clear trend in how the feed concentration affects the concentration of TEG in the permeate, and it is therefore not possible to say anything definite about it. A reason for why this trend is not clear could be due to the fact that TEG has a higher dew point than the water and it is therefore

possible that the TEG is condensed on the walls of the tubes that lead from the membrane to the sampleholder as well as in the sintered plate under the membrane. When these droplets form the amount of TEG in some samples can be lower than they should while others get a higher concentration because droplets from previous tests is introduced to later samples. When removing the membrane at the end of the tests the sintered plate felt oily and it can therefore be assumed that the TEG was condensed in the sintered plate leading to a large error in the concentration measurements.

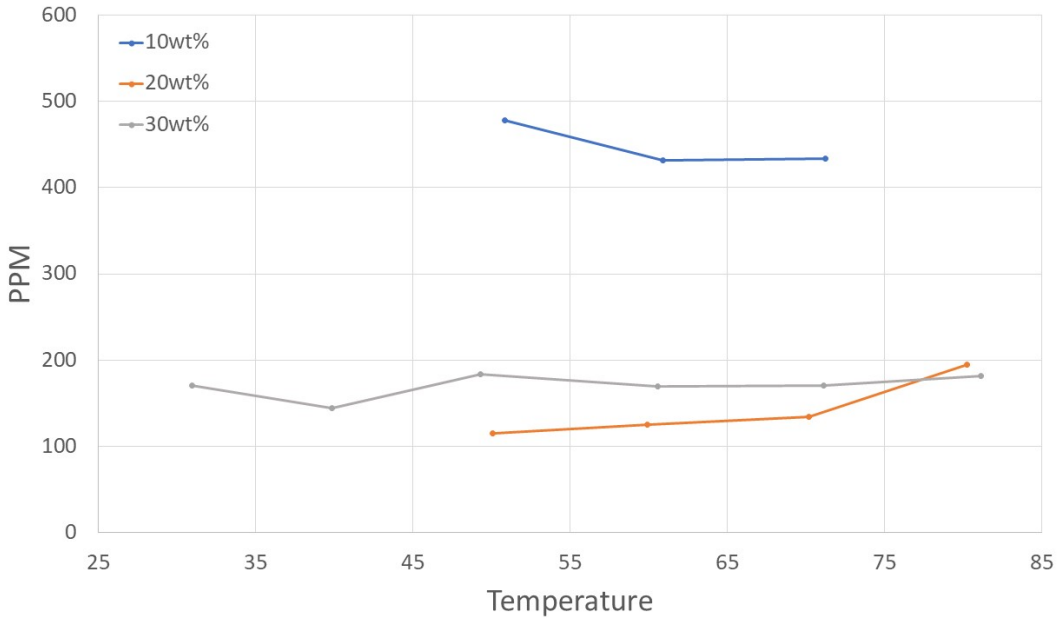

Figure 4.7.2: Graph of the concentration of TEG in the permeate measured in PPM with respect to temperature.

If the TEG is condensing in the sintered plate and the tubes as stated above it will also affect the flux measurements since the flux of TEG can be either increased or decreased based on if the TEG condenses or is released from the sintered plate during the test. The concentration of TEG in the permeate is however quite low as can be seen in figure 4.7.2, the highest concentration is at around $477PPM$ which in turn gives a weight fraction of TEG in the permeate of $4{,}7 \cdot 10^{-6}$ which indicates that it has a minimal effect on the actual weight of the permeate and therefore has a minimal effect on the flux calculations. This can also be seen in figure 4.7.3 where both the total flux and the water flux is plotted against the feed water concentration.

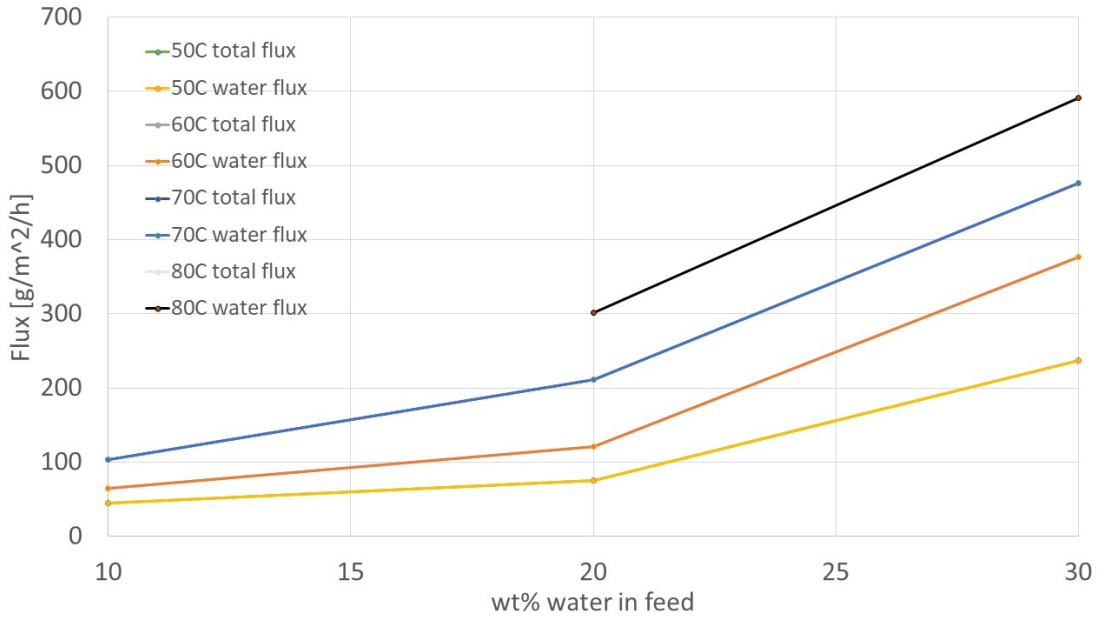

Figure 4.7.3: Plot of both total flux and water flux through the membrane at different temperatures and different weight fractions of water in the feed.

As seen in figure 4.7.3 the water flux and the total flux remains the same for every feed composition and temperature since the graphs overlaps entirely. When looking at the separation factor calculated from the concentration measurements the results are still quite good since the lowest value calculated is 111365,26 which is quite high. This is however as stated above probably not a correct measurement since the TEG might have condensed in the sintered plate and on the walls of the tubes leading to the sampleholder. The fact that the calculated separation factor is so high is an indication that there has not been an increase in TEG concentration in the samples due to droplets beeing released from the sintered plate and the tube walls, but instead the TEG has constantly been building up in these places.

The permeance of water and TEG was calculated using the concentration values from the gas chromatograph, which means that the TEG values suffers from the same problems as the TEG flux calculations. The TEG permeance is therefore not included here. The water permeance can be seen in figure 4.7.4 and should be approximately the correct values since the TEG concentration is not high enough to cause a large error in the water measurements.

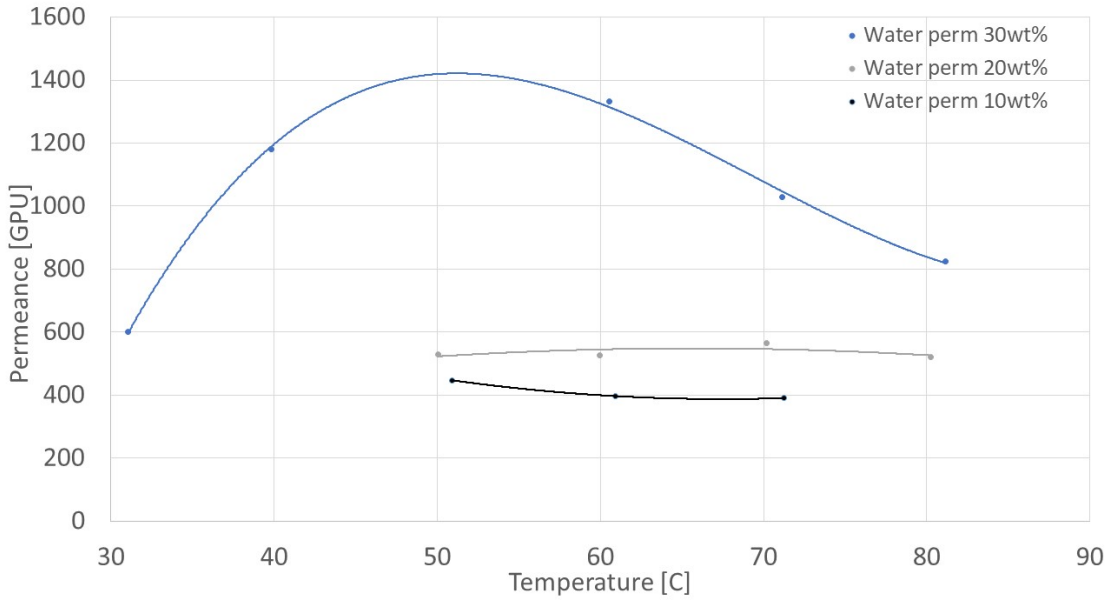

Figure 4.7.4: Graph of the calculated water permeance in GPU with respect to temperature and at different feed water concentrations.

As seen in figure 4.7.4 the permeance of water is almost constant at feed water concentrations of $20wt\%$ and $10wt\%$ with a small decrease. At $30wt\%$ it is however changing quite drastically with temperature. When looking at the arrhenius equation 2.5.18 the permeability should be strictly increasing or decreasing with the temperature depending on the value of the activation energy E_J. The reason for the abnormality in the permeance at $30wt\%$ is currently unknown, but is probably due to a measurement error or an error when using the pervaporation module.

Conclusion

The purpose of this thesis was to determine if polybenzimidazole (PBI) is a suitable polymer for the dehydration of triethylene glycol (TEG). A composite membrane with a porous polypropylene support with a thickness of $25\mu m$ and a $2{,}5\mu m$ thick layer of PBI was therefore prepared and tested in a pervaporation setup.

The SEM picures given in figure 4.4.1 showed that the thickness of the membrane was quite consistent over the membrane at $2{,}5 \pm 0{,}2\mu m$.

From the results of the FTIR samples it can be concluded that the membrane was still containing water after the preparation process used for the selfstanding PBI membrane. This shows that the membrane should be dried for a longer time to remove all of the water from the matrix. This is however not a large problem in this project since the membrane is going to be in contact with an aqueous solution for the tests and a certain amount of water absorption in the membrane is not possible to avoid.

The thermogravimetric analysis showed that the boiling and washing of the membrane is necessary for the removal of the LiCl and the DMAc from the membrane matrix since it is clear that the membrane contained LiCl and DMAc before these steps and not after.

When looking at the flux through the membrane with respect to the feed composition at different temperatures the results were quite promising. The total flux increased by a smaller amount from $10wt\%$ to $20wt\%$ than from $20wt\%$ to $30wt\%$ and the flux ranged from $14{,}78[\frac{g}{m^2h}]$ to $590{,}61[\frac{g}{m^2h}]$ at $30wt\%$ water in the feed. This shows that the the membrane has a high rate of permeation which means that the membrane can be more compact when implementing it on an industrial scale since the membrane will require a smaller surface area.

There were some problems that arose when the permeate TEG concentration was tested by the use of a gas chromatograph. The concentrations did not show a consistent pattern or trend with the temperature or the feed water concentration. A possible reason for this was determined to be the sintered plate under the mem-

brane in the pervaporation setup and the tubes leading to the sampleholder where the TEG could possibly condense in the plate and at the walls of the tubes and therefore give a lower or higher amount of TEG in the samples and therefore not give an accurate measurement of the permeation rate of the TEG. For further testing the permeation setup therefore needs to be modified to prevent this TEG buildup and get a good measurement of the TEG concentration. Even though the TEG measurements were highly inacurate none of the measurements consitituted more than a $2{,}26 \cdot 10^{-5}$ mole fraction which is not a large concentration. This was seen in figure 4.7.3 where the water flux is practically the same as the total flux through the membrane, which means that the membrane has good separation properties when separating water from TEG. Exactly how good the separation is is however difficult to determine. This can also be seen from the value of the separation factor that was calculated where the lowest separation factor, 111365,26, is still quite high. This is however just an indication since the actual separation factor is impossible to find without an accurate TEG concentration.

As seen in figure 4.7.4 the $10wt\%$ and $20wt\%$ showed a good water permeance with the $10wt\%$ curve showing a permeance around $447GPU$ and $390GPU$ while the $20wt\%$ was between $564GPU$ and $520GPU$. The $30wt\%$ however showed what is most likely a large measurement error. A permeance of around 500 is not a high permeance and the and could be seen as an indication that the membrane is not a viable option for dehydration of TEG by pervaporation. More tests is however needed to be able to say anything conclusively on this due to the fact that the TEG concentration was so inconsistent and that the permeance at $30wt\%$ is quite likely a measurement error.

Bibliography

[1] Dalane K, Dai Z, Mogseth G, Hillestad M, Deng L. Potential applications of membrane separation for subsea natural gas processing: A review; 2017.

[2] Mokhatab S, Poe WA, Mak JY. Handbook of Natural Gas Transmission and Processing: Principles and Practices: Third Edition; 2015.

[3] Mokhatab S, Poe WA, Mak JY, Mokhatab S, Poe WA, Mak JY. Chapter 7 – Natural Gas Dehydration. In: Handbook of Natural Gas Transmission and Processing; 2015. p. 223–263.

[4] Baker RW, Lokhandwala K. Natural gas processing with membranes: An overview; 2008.

[5] Yang X, Wang R, Fane AG, Tang CY, Wenten IG. Membrane module design and dynamic shear-induced techniques to enhance liquid separation by hollow fiber modules: A review; 2013.

[6] Josefsen N. Subsea regeneration of triethylene glycol (TEG) for natural gas dehydration. Norwegian University of Science and Technology; 2017. Available from: `http://hdl.handle.net/11250/2469435`.

[7] Gandhidasan P. Parametric analysis of natural gas dehydration by a triethylene glycol solution. Energy Sources. 2003;.

[8] Mokhatab S, Poe W. Handbook of Natural Gas Transmission and Processing; 2012.

[9] Koros WJ, Zhang C. Materials for next-generation molecularly selective synthetic membranes. Nature Materials. 2017;.

[10] Jyoti G, Keshav A, Anandkumar J. Review on Pervaporation: Theory, Membrane Performance, and Application to Intensification of Esterification Reaction; 2015.

[11] Figoli A, Santoro S, Galiano F, Basile A. Pervaporation membranes: Prepa-

ration, characterization, and application. In: Pervaporation, Vapour Permeation and Membrane Distillation: Principles and Applications; 2015. .

[12] Geankoplis CJ. Transport Processes and Unit Operations (Geankoplis).pdf; 2003. Available from: http://www.getcited.org/pub/103012079.

[13] Wijmans JG, Baker RW. The solution-diffusion model: a review; 1995.

[14] Laciak DV, Langsam M. Gas Separations with Polymer Membranes. m, Corporate Science and Technology Center. 2000;p. 1725–1738.

[15] Wijmans JGH, Baker RW. The Solution-Diffusion Model: A Unified Approach to Membrane Permeation. In: Materials Science of Membranes for Gas and Vapor Separation; 2006. .

[16] Mulder M. Basic Principles of Membrane Technology Second Edition; 1996. Available from: http://linkinghub.elsevier.com/retrieve/pii/037673889285058Q%5Cnhttp://scholar.google.com/scholar?hl=en&btnG=Search&q=intitle:basic+principles+of+membrane+technology#1%5Cnhttp://scholar.google.com/scholar?hl=en&btnG=Search&q=intitle:Basic+principles+of+me.

[17] Wang Y, Chung TS, Neo BW, Gruender M. Processing and engineering of pervaporation dehydration of ethylene glycol via dual-layer polybenzimidazole (PBI)/polyetherimide (PEI) membranes. Journal of Membrane Science. 2011;.

[18] Sparkman OD, Penton Z, Kitson FG. Gas Chromatography and Mass Spectrometry: A Practical Guide; 2011.

[19] Musto P, La Manna P, Moon JD, Galizia M, Freeman BD. Infrared Spectroscopy of Polybenzimidazole in the Dry and Hydrate Forms: A Combined Experimental and Computational Study. ACS Omega. 2018;.

[20] Prime RB, Bair HE, Vyazovkin S, Gallagher PK, Riga A. Thermogravimetric Analysis (TGA). In: Thermal Analysis of Polymers: Fundamentals and Applications; 2008. .

Appendix

A Risk assessment

Below is a detailed risk-assessment of the work done in the labs for this project following the guidelines of NTNU. The risk assessment is done based on NTNUs guidelines and the MSDS datasheets for the chemicals used in this project.

Detaljert Risikorapport

ID	23830	**Status**	**Dato**
Risikoområde	Risikovurdering: Helse, miljø og sikkerhet (HMS)	Opprettet	10.11.2017
Opprettet av	Askild Johannes Balchen Lønning	Vurdering startet	
Ansvarlig	Askild Johannes Balchen Lønning	Tiltak besluttet	
		Avsluttet	

Risikovurdering:

EEART, Project, 2018, Askild Lønning

Gyldig i perioden:
8/24/2018 - 1/10/2019

Sted:
3 - Gløshaugen / 314 - Kjemi 4 / 1020 - 2. etasje / 4.218 / 4.216 / 4.217 / Kjemi 4 / 0510 - Kjeller / 4.010/ Hall C

Mål / hensikt
Risk assessment of master project.

Bakgrunn
Risk assessment of the work done during the master project in the labs 4.218, 4.217, 4.216, 4.010 and Hall C

Beskrivelse og avgrensninger
Chemicals:
- Polymeric materials. (AF2400, Porous Polypropylene, PBI and PAN)
- Solvents (FC-72)
- Triethylene Glycol

Risk assessments of the apparatuses used in this projec thas been risk assessed previously and the risk assessments are included in the references.

Forutsetninger, antakelser og forenklinger
The MSDS for all of the chemicals used in this project has been analyzed and no hazzards has been linked to working with these chemicals.

Vedlegg
[Ingen registreringer]

Referanser
Room risk assessment K4 010(https://avvik.ntnu.no/Risk/EditRiskAssessment?id=12203&showActions=false&readOnlyMode=True)
Room risk assessment K4 216(https://avvik.ntnu.no/Risk/EditRiskAssessment?id=12202&showActions=false&readOnlyMode=True)
EEART, Instrument, K4.010, TGA (Thermoegravimetric analysis) Netzsch(https://avvik.ntnu.no/Risk/EditRiskAssessment?id=7004&showActions=false&readOnlyMode=True)
EEART, Instrument, K4.010, DSC (Differential Scanning Calorimeter) Netzsch(https://avvik.ntnu.no/Risk/EditRiskAssessment?id=7002&showActions=false&readOnlyMode=True)
Membrane Preparation Procedure(https://avvik.ntnu.no/Risk/EditRiskAssessment?id=346&showActions=false&readOnlyMode=True)
EEART Instrument - Hall C - Pervaporation setup (permeation rig)(https://avvik.ntnu.no/Risk/EditRiskAssessment?id=326&showActions=false&readOnlyMode=True)
EEART, Engineer, Gøril Flatberg(https://avvik.ntnu.no/Risk/EditRiskAssessment?id=164&showActions=false&readOnlyMode=True)

B Pervaporation results

Temperature $[C]$	Flux $[\frac{g}{m^2h}]$	Y_{H_2O} [-]	Y_{TEG} [-]
31.06	14.78	–	–
31.08	30.85	0.9999	$3.97 \cdot 10^{-6}$
30.99	39.48	0.9999	$1.89 \cdot 10^{-6}$
39.83	96.55	0.9999	$8.05 \cdot 10^{-7}$
39.86	102.60	0.9999	$1.70 \cdot 10^{-6}$
39.85	144.15	0.9999	$1.59 \cdot 10^{-6}$
49.30	206.60	–	–
49.31	264.68	0.9999	$2.42 \cdot 10^{-5}$
49.34	210.25	0.9999	$2.02 \cdot 10^{-5}$
49.35	268.73	0.9999	$2.11 \cdot 10^{-5}$
60.55	372.65	0.9999	$2.26 \cdot 10^{-5}$
60.55	399.64	0.9999	$1.76 \cdot 10^{-5}$
60.55	356.78	0.9999	$3.15 \cdot 10^{-6}$
71.11	493.49	0,9999	$1.62 \cdot 10^{-7}$
71.16	496.90	0.9999	$1.74 \cdot 10^{-7}$
71.13	438.78	0.9999	$2.01 \cdot 10^{-7}$
81.17	592.97	0.9999	$2.01 \cdot 10^{-7}$
81.13	588.28	0.9999	$1.90 \cdot 10^{-7}$
81.07	590.61	0.9999	$1.79 \cdot 10^{-7}$

Table B.1: Results with PBI membrane and a solution of $30wt\%$ water in TEG as feed

Temperature $[C]$	Flux $[\frac{g}{m^2h}]$	Y_{H_2O} [-]	Y_{TEG} [-]
28.55	7.15	–	–
28.56	5.51	–	–
50.06	75.97	0.9999	$8.77 \cdot 10^{-6}$
50.09	75.55	0.9999	$1.44 \cdot 10^{-5}$
50.07	73.20	0.9999	$8.06 \cdot 10^{-7}$
59.71	143.02	0.9999	$1.48 \cdot 10^{-6}$
60.42	85.64	0.9999	$9.74 \cdot 10^{-6}$
59.65	135.33	0.9999	$1.032 \cdot 10^{-5}$
70.19	189.26	0.9999	$1.06 \cdot 10^{-7}$
70.22	229.11	0.9999	$1.16 \cdot 10^{-7}$
70.16	214.63	0.9999	$2.02 \cdot 10^{-7}$
80.23	252.15	0.9999	$2.05 \cdot 10^{-7}$
80.26	305.63	0.9999	$2.00 \cdot 10^{-7}$
80.25	347.31	0.9999	$2.31 \cdot 10^{-7}$

Table B.2: Results with PBI membrane and a solution of $20wt\%$ water in TEG as feed

Temperature $[C]$	Flux $[\frac{g}{m^2h}]$	Y_{H_2O} [-]	Y_{TEG} [-]
29.01	21.61	–	–
29.33	23.52	–	–
29.02	24.70	–	–
39.85	42.19	–	–
39.83	41.45	–	–
39.79	41.87	–	–
50.81	49.50	–	–
50.86	47.70	–	–
50.88	50.71	–	–
50.89	46.68	0.9999	$4.49 \cdot 10^{-7}$
50.88	43.77	0.9999	$3.96 \cdot 10^{-7}$
50.88	43.37	0.9999	$6.82 \cdot 10^{-7}$
60.99	65.10	0.9999	$9.69 \cdot 10^{-6}$
60.93	66.58	0.9999	$4.76 \cdot 10^{-6}$
60.78	63.87	0.9999	$5.28 \cdot 10^{-6}$
71.21	108.09	0.9999	$5.02 \cdot 10^{-7}$
71.19	103.12	0.9999	$5.85 \cdot 10^{-7}$
71.32	100.09	0.9999	$3.01 \cdot 10^{-7}$

Table B.3: Results with PBI membrane and a solution of $10wt\%$ water in TEG as feed

Temperature $[C]$	Flux $[\frac{g}{m^2h}]$
30.49	348.33
31.33	354.94
29.98	345.20
40.55	550.47
40.56	545.43
40.56	581.17
50.04	822.39
50.04	811.03
50.01	797.97
59.65	1173.64
59.66	1158.38
59.62	1148.07
69.83	1668.52
69.77	1663.24
69.83	1689.63
80.86	2276.73
80.92	2285.48
81.05	2288.98

Table B.4: Results with PBI membrane and pure water in the feed

C Results from gas chromatograph

Temperature [C]	Feed weight fraction	TEG concentration [PPM]
50,89	0,1	40,54
50,88	0,1	34,87
50,88	0,1	54,92
60,99	0,1	412,71
60,93	0,1	425,04
60,78	0,1	457,71
71,21	0,1	480,04
71,19	0,1	543,40
71,32	0,1	276,65
31,08	0,3	345,33
30,99	0,3	170,13
39,83	0,3	69,38
39,86	0,3	148,02
39,85	0,3	140,11
49,31	0,3	202,72
49,34	0,3	170,12
49,35	0,3	177,00
60,55	0,3	190,83
60,55	0,3	148,55
60,55	0,3	53,87
71,11	0,3	154,88
71,16	0,3	164,89
71,13	0,3	192,83
81,17	0,3	193.60
81,13	0,3	182,93
81,07	0,3	168,52
50,06	0,2	125,99
50,09	0,2	122,16
50,07	0,2	98,20
59,71	0,2	126,07
60,42	0,2	119,73
59,65	0,2	129,21
70,19	0,2	103,73
70,22	0,2	109,01
70,16	0,2	190,30
80,23	0,2	190,30
80,26	0,2	187,88
80,25	0,2	207,24

Table C.1: The concentration of TEG in the permeate at different feed water composition and temperature in [PPM] measured by gas chromatography.

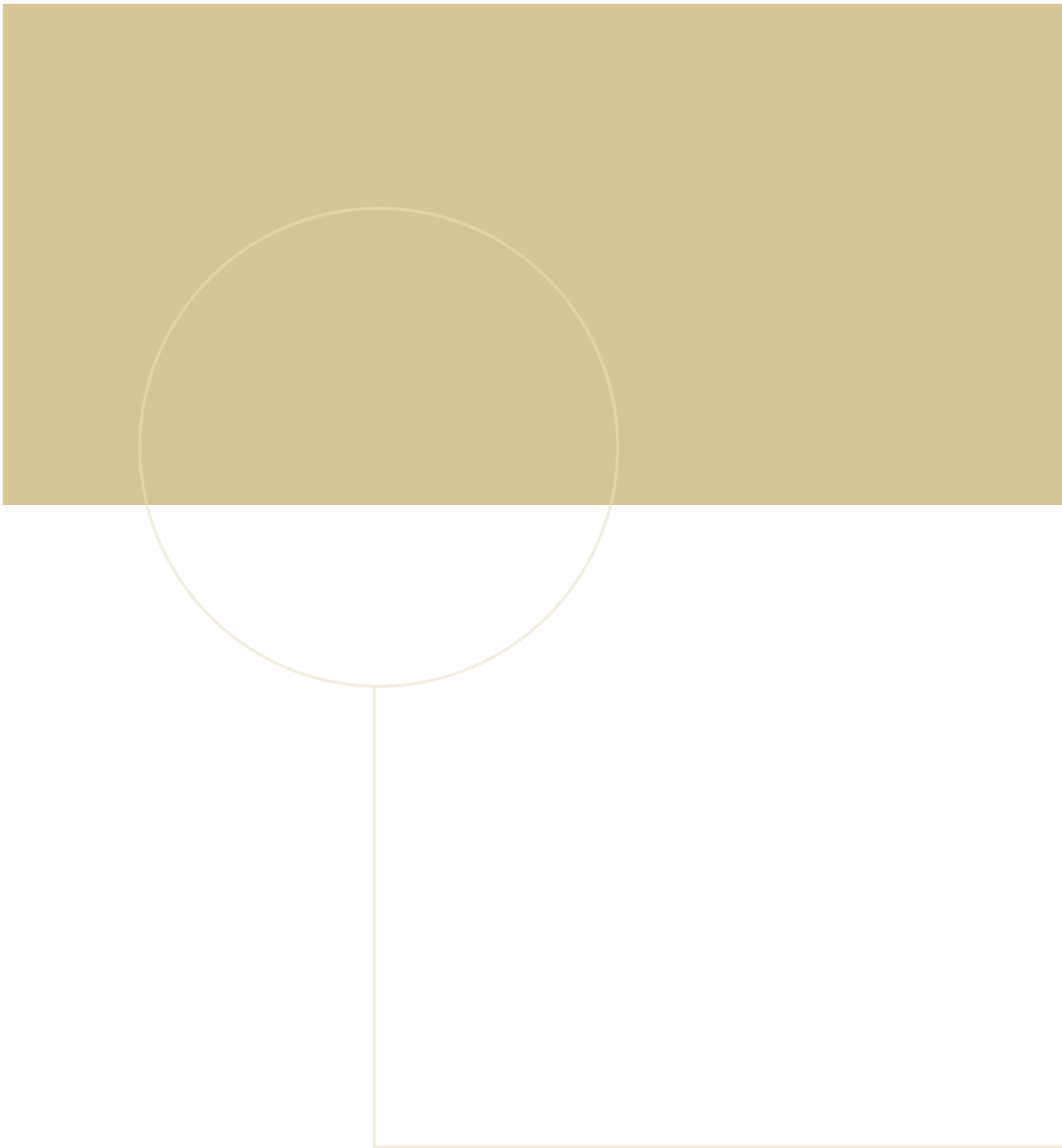

NTNU
Norwegian University of
Science and Technology